OPEN ACCESS
JOURNAL OF ADVANCED DIELECTRICS
Vol. 11, No. 4 (2021) 2150022 (10 pages)

DOI: 10.1142/S2010135X21500223

Assessment of dielectric strength and partial discharges patterns in nanocomposites insulation of single-core power cables

Ahmed Thabet[*,†,§] and M. Fouad[‡]

[*]*Nanotechnology Research Center*
Electrical Engineering Dept.
Faculty of Energy Engineering
Aswan University, Aswan, Egypt

[†]*Electrical Engineering Dept.*
College of Engineering and Information Technology
Buraydah Colleges, KSA

[‡]*Hydro Power Plant Generation Company*
Nag Hammadi Hydro Power Plant, Qena, Egypt

[§]athm@aswu.edu.eg

Received 18 May 2021; Revised 30 June 2021; Accepted 14 July 2021; Published 6 September 2021

Nanoparticles succeeded to enhance the dielectric properties of industrial insulation but the presence of voids inside the power cable insulation still leads to formation high electrical stress inside power cable insulation material and collapse. In this paper, the dielectric strength of new design nanocomposites has been deduced as experimental work done to clarify the benefit of filling nanoparticles with different patterns inside dielectrics. Also, it has been studied the effect of electrical stress distribution in presence of air, water and copper impurities with different shapes (cylinder, sphere and ellipse) inside insulation of single core. In simulation model, it has been used finite element method (FEM) for estimating the electrostatic field distribution in power cable insulation. It has been applied new strategies of nanotechnology techniques for designing innovative polyvinyl chloride insulation materials by using nanocomposites and multi-nanocomposites. Finally, this research succeeded to remedy different partial discharges (PD) patterns according to using certain types and concentrations of nanoparticles.

Keywords: Partial discharges; dielectric strength; single core; cables; FEM; nanocomposites; nanoparticles.

1. Introduction

Most of the industrial insulations are not 100% exemplary in nature and always contain some impurity. During the manufacturing process, the presence of (air–water) bubbles in the insulating material is one of the causes for making the insulation insufficient.[1,2] Partial discharge occurs in places which their electric field intensity is higher than tolerable value of insulator in a power cable, the main reason for dielectric failure, is occurrence of partial discharge inside insulation cavities. When electric strength of a cavity is low, applied electric field to cavity can lead to breakdown in cavity and also solid insulator. This type of discharges leads to local dielectric breakdown in cables. Furthermore, other factors such as electric discharges. Impurities, roughness and space charges can also be affecting on cable insulator life time.[3] The ionization and incident of partial discharges within the voids would cause abrasion and local decay of the insulation, which leads to a complete failure of the power cable.[4] Of course, the partial discharge occurs in places that their electric field intensity is higher than accepted value of insulator in a power cable. Finite Element Method (FEM) has been used to study bubbles effect in high voltage power cable insulations as a basic method. It is known that the field intensity rises the breakdown strength of air in void, then partial discharge takes place. However, once the PD starts inside the high voltage power equipment, it continues for a long time if it is not taken care of and finally degrades quality of insulation properties. In recent years, the progress of nanotechnology science is fast to innovate new insulation materials that have advanced physical and electrical properties.[5–8] Recently, individual and multiple nanoparticles techniques investigated the best trends for enhancing the electric and dielectric properties; therefore, the new nanocomposites have been having the capabilities for accepting the sufficient effective electric and dielectric properties of base matrix dielectric material.[9–14] The aim of this paper is enhancing insulation performance of single-core power cables that are exposed to manufacture defects like air voids, water voids, impurities,

[§]Corresponding author.

etc. Thus, this paper has been studied the electrical stress distribution in presence of different shapes of voids (rectangle–circle–ellipse) in the case of using individual and multiple nanoparticles techniques to insulation of single-core power cables. The proposed model takes into account the presence of air, water and copper impurities with different shapes (cylinder, sphere and ellipse) inside insulation of single-core individual and multi-nanocomposites system in the form of interphase regions. The electrostatic field distribution and partial discharges characteristics in the new industrial nanocomposites materials have been discussed based on charge simulation method (CSM). Also, this research success to specify optimal types and concentrations of individual and multiple nanoparticles for enhancing polymeric insulations of single-core power cables.

2. Simulation Model

It is known by the theory that in a single-core cable of having (r) radius of conductor and (R) inner radius of insulation, the potential gradient (g) at a distance (x) from the center of the conductor within the dielectric material is

$$g = \frac{q}{2\pi\varepsilon x} = \xi x, \tag{1}$$

where ξx is the electric field intensity, q is the charge per unit length, ε is the permittivity of the dielectric material. So, the potential of the conductor will be

$$V = -\int_R^r \xi x \cdot dx, \tag{2}$$

$$= \int_R^r \frac{q}{2\pi\varepsilon x}.dx, \tag{3}$$

since $\frac{q}{2\pi\varepsilon x}\xi x$ (from Eq. (1)). So,

$$\xi x = \frac{V}{x \log e^{\frac{R}{r}}}. \tag{4}$$

Here, x is the only variable in the equation; the maximum stress in dielectric material occurs at the minimum value of the radius (here, $x = r$).[4] So,

$$\xi x = \frac{V}{r \log e^{\frac{R}{r}}}. \tag{5}$$

But all the times irregular problem geometry for void is so complicated that analytical solution is so hard. Due to this reason, researches tried to find new calculating methods to obtain electric field. FEM is chosen for computation use. Electric field equations solution by this method is based on Maxwell equations with boundary conditions.

Fig. 1. Cross-section of single-core power cable with (cylinder–sphere–ellipse) voids.

3. Configuration and Specifications

In this research, it has been investigated single-core power cable configuration as shown in Fig. 1. The model configuration is setup according to standard dimensions designed by NEXANS Energy Networks Company, Design Standards 6622–BS 7835.[15] Table 1 illustrates the specifications of this case study of single-core power cable, whatever the voids are located between the conductor surface and the insulation outer surface. Moreover, the void diameter is considered 1 mm located between the conductor surface and the insulation inner surface.[15–17] Finite Element Methods Magnetics (FEMM) software is used for this simulation. Finite Element

Table 1. Configuration of single-core cable.[15–17]

Specification	Rating
Rated voltage (kV)	11 kV
Number core	1
Nominal cross-sectional area	150 mm^2
Diameter over conductor	14.3 mm
Approximate diameter over insulation	22.2 mm
Approximate overall diameter	38 mm
Insulation dielectric constant (PVC)	3
Water permittivity	81
Air permittivity	1
Copper impurity permittivity	5.6
Radius of bubble	0.5 mm

Method Magnetics (FEMM) software is a finite element package. FEMM software is used for solving two-dimensional planar and axisymmetric problems in electrostatics, current flow, heat flow and low-frequency magnetic.[18,19]

4. Material Design and Fabrication

Power law relationships are used in dielectric modeling of composite systems by using individual nanoparticles; so that the composite system has three components as follows: matrix, nanoparticle and interphase region.[20–22] Furthermore, the interphase region is dependent upon the nanoparticle volume fraction, the nanoparticle surface area and the thickness of the interphase region surrounding each nanoparticle particle.[19] Whatever, it has been proposed a multi-nanoparticles technique for developing the electric and dielectric properties of polymer.[23] Estimation of interphase thickness is further developed based on Refs. 24–27. Figure 2 shows the nanoparticles come close together, and the interphase regions surrounding each nanoparticle begin to overlap. Recently, it has been studied theoretical and experimental studies for enhancing the electrical properties and variant industrial insulation materials for electrical applications.[28–31] Recent researches refer to the effective dielectric constant of the inclusion and interphase that has been expressed for multiple nanocomposite model that contains an interphase region.[20,21,31]

$$\varepsilon_{\text{effj}}^{\beta} = \varphi_j \varepsilon_j^{\beta} + \varphi_{\text{phij}} \varepsilon_{\text{phij}}^{\beta} + \varphi_{\text{effi}} \varepsilon_{\text{effi}}^{\beta}, \tag{6}$$

where φ_j is the volume fraction of second nanoparticle component of the multi-composite system, φ_{phij} is the volume fraction of the interphase region component of the multi-composite system, φ_{effi} is the volume fraction of the initial matrix component of the multi-composite, $\varepsilon_{\text{effj}}$ is the dielectric permittivity of the multi-composite system, ε_j is the second nanoparticle permittivity of the multi-composite system, $\varepsilon_{\text{phij}}$ is the interphase permittivity of the multi-composite system and $\varepsilon_{\text{effi}}$ is the dielectric permittivity of the individual nanocomposites system. The second nanoparticle volume fraction of Eq. (6), φ_j, is directly measured for a given composite system. The matrix volume fraction is given by $\varphi_{\text{effi}} = (1 - \varphi_j - \varphi_{\text{phij}})$. The interphase volume fraction of multi-composite system, φ_{phij}, is estimated as follows:

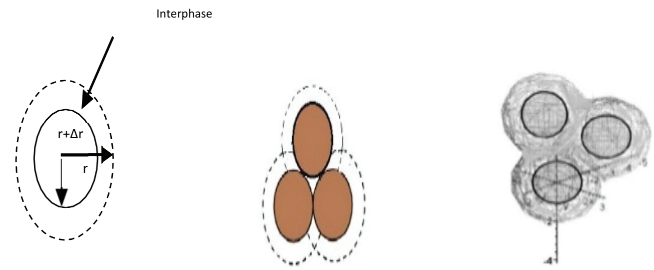

Fig. 2. Interphase region surrounding the multi-nanoparticle particles in multi-nanocomposites system.

$$\varphi_{\text{phij}} = (1 - F)\cdot(S_j \Delta r)\rho_j \varphi_j, \tag{7}$$

where S_j is the specific surface area of second nanoparticle (measured in m^2/g), ρ_j is the density of second nanoparticle (measured in g/m^3), Δr is the thickness of the interphase region and F is an overlap probability function.

Polyvinyl Chloride (PVC) is the most widely used of any of cables, thermoplastics, polymerized vinyl chloride, which is produced from ethylene and anhydrous hydrochloric acid. PVC is stronger and more rigid than other general-purpose thermoplastic materials. Polyvinyl chloride is basically tough and strong, resist water and abrasion, and are excellent electrical insulators. Nanoparticles are used to enhance the physical and electric characterizations of polymers as design and investment the nanodielectrics.[21,22] Aluminum Oxide (Al_2O_3) is strong high heat-resistance, very stable, high hardness, high mechanical strength and electrical insulator. Zinc Oxide (ZnO) is used in paints, coatings, cross linker of rubber and

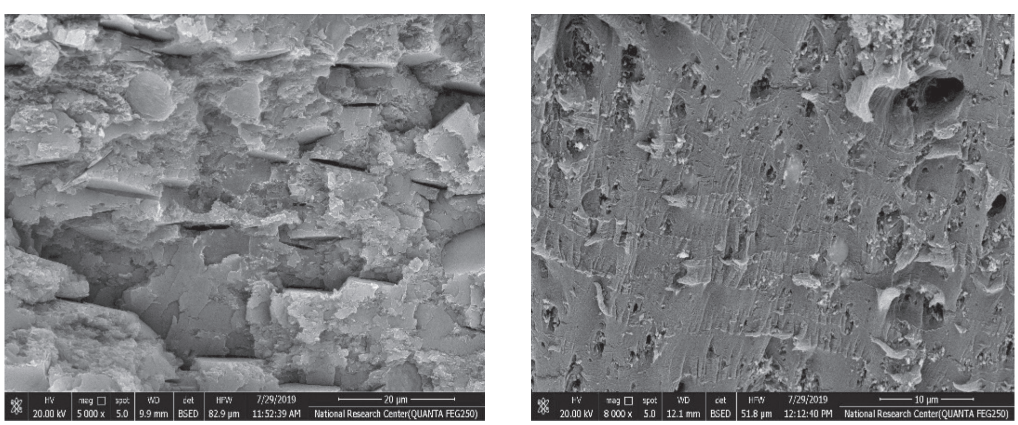

(a) Clay/PVC nanocomposites (b) ZnO/PVC nanocomposites

Fig. 3. SEM measurements for nanoparticles distribution in PVC.

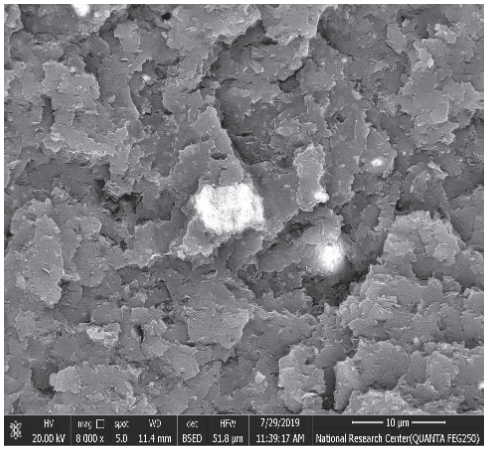

(c) (Clay + $BaTiO_3$)/PVC nanocomposites

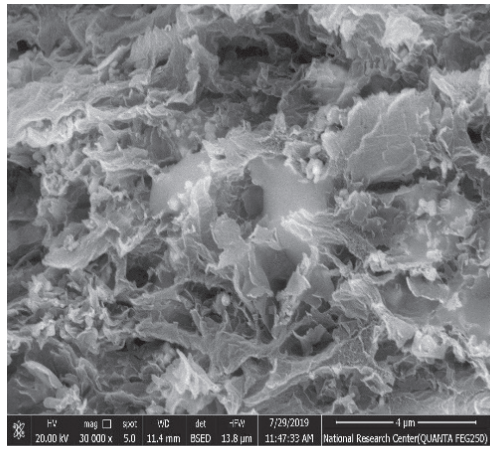

(d) (ZnO + $BaTiO_3$)/PVC nanocomposites

Fig. 3. (*Continued*)

sealants, Magnesium Oxide (MgO) has high thermal conductivity and low electrical conductivity, whatever Barium titanate ($BaTiO_3$) is a dielectric ceramic used for capacitors.

4.1. *Test sample preparation*

Spherical nanoparticles characterization shape (Dia.: 50 nm) have been used in our test sample preparation; the penetration of nanoparticles inside polyvinyl chloride has been detected by using Scanner of Electron Microscopic "SEM" images as shown in Fig. 3.

4.2. *Nanometric materials characterization*

Clay is the best filler as a catalyst among nanoparticles industrial materials and has a costless feature, whatever fumed silica nanoparticles are fluffy white powders with an extremely low density marketed. Polyvinyl chloride is a commercially available material already in use in the manufacturing of high-voltage HV industrial products and their properties are detailed in Table 2. Nanocomposite Polymer: Preparation of studied nanocomposites polymers has been used SOL-GEL method fabrication.[32–35] Measurement Devices: HIOKI 3522-50 LCR Hi-tester device measured characterization of nanocomposite insulation industrial materials. All fabricated polyvinyl chloride nanocomposites and multi-nanocomposites have been characterized in this research as shown in Table 3.

5. HV Breakdown Measurements

HI-POT TESTER Model ZC2674 device has been used for experiment uniform and nonuniform electric field distribution through the thickness of insulation layer with different nanocomposite materials. In the case of uniform electric

Table 2. Dielectric constant of polyvinyl chloride nanocomposites and multi-nanocomposites materials.

Nanoparticles and pure material	Dielectric constant
Clay	2
$BaTiO_3$	3.8
ZnO	1.8
PVC	3
Nanocomposites	**Dielectric constant**
5 wt.% Clay/PVC	2.801
(5 wt.% Clay + 7 wt.% ZnO)/PVC	2.608
(5 wt.% Clay + 12 wt.% ZnO)/PVC	2.484
(5 wt.% Clay + 7 wt.% $BaTiO_3$)/PVC	2.872
(5 wt.% Clay + 12 wt.% $BaTiO_3$)/PVC	2.924
(5 wt.% Clay + 7 wt.% Al2O_3)/PVC	4.871
(5 wt.% Clay + 12 wt.% Al_2O_3)/PVC	6.62
5 wt.% ZnO/PVC	2.831
(5 wt.% ZnO + 7 wt.% Clay)/PVC	2.608
(5 wt.% ZnO + 12 wt.% Clay)/PVC	2.47
(5 wt.% ZnO + 7 wt.% $BaTiO_3$)/PVC	2.901
(5 wt.% ZnO + 12 wt.% $BaTiO_3$)/PVC	2.95
(5 wt.% ZnO + 7 wt.% Al_2O_3)/PVC	4.898
(5 wt.% ZnO + 12 wt.% Al_2O_3)/PVC	6.638
5 wt.% $BaTiO_3$/PVC	3.084
(5 wt.% $BaTiO_3$ + 7 wt.% Clay)/PVC	2.807
(5 wt.% $BaTiO_3$ + 12 wt.% Clay)/PVC	2.736
(5 wt.% $BaTiO_3$ + 7 wt ZnO)/PVC	2.901
(5 wt.% $BaTiO_3$ + 12 wt.% ZnO)/PVC	2.888

Table 3. Stress distribution in cable insulation with different air voids.

Materials	E_{max} within cable insulation (V/m)	E_{max} within air cylinder void (V/m)	E_{max} within air sphere void (V/m)	E_{max} within air ellipse void (V/m)
Pure PVC	5.24E+05	9.13E+05	4.58E+05	5.12E+05
5 wt.% Clay/PVC	5.31E+05	8.84E+05	4.58E+05	4.99E+05
(5 wt.% Clay + 7 wt.% ZnO)/PVC	5.39E+05	8.55E+05	4.57E+05	4.85E+05
(5 wt.% Clay + 12 wt.% ZnO)/PVC	5.45E+05	8.35E+05	4.57E+05	4.76E+05
(5 wt.% Clay + 7 wt.% $BaTiO_3$)/PVC	5.28E+05	8.95E+06	4.58E+05	5.04E+05
(5 wt.% Clay + 12 wt.% $BaTiO_3$)/PVC	5.26E+05	9.02E+05	4.58E+05	5.07E+05
5 wt.% ZnO/PVC	5.30E+05	8.89E+05	4.58E+05	5.01E+05
(5 wt.% ZnO + 7 wt.% Clay)/PVC	5.39E+05	8.55E+05	4.57E+05	4.85E+05
(5 wt.% ZnO + 12 wt.% Clay)/PVC	5.46E+05	8.33E+05	4.57E+05	4.75E+05
(5 wt.% ZnO + 7 wt.% $BaTiO_3$)/PVC	5.27E+05	8.99E+06	4.58E+05	5.05E+05
(5 wt.% ZnO + 12 wt.% $BaTiO_3$)/PVC	5.25E+05	9.06E+05	4.58E+05	5.08E+05

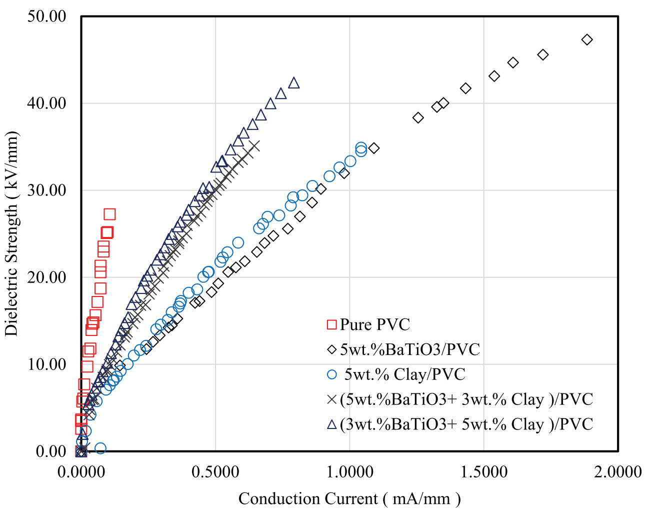

Fig. 4. Dielectric strength of nanocomposite insulation material containing Clay and $BaTio_3$ nanoparticles under uniform electric fields.

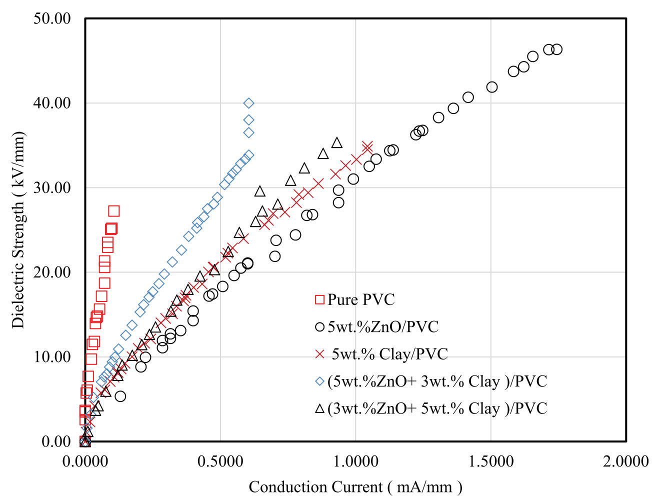

Fig. 5. Dielectric strength of nanocomposite insulation material containing Clay and ZnO nanoparticles under uniform electric fields.

fields measurements, it has been used two copper cylindrical electrodes (Dia. 20 mm) that are sandwiched the test sample (Dia. 35 mm). In the case of nonuniform electric fields, insulation test sample sandwiched between the tip electrode pin (Dia. less than 0.5 mm) and flat copper plate. Figures 4–6 show the measurements of breakdown characterization of pure and nanocomposite insulation industrial materials under uniform electric fields by using Hi-tester device. It has been obvious that adding individual nanoparticles (Clay, ZnO and $BaTiO_3$) raising maximum dielectric strength of polyvinyl chloride, especially, in the case of adding two different types of nanoparticles together in polyvinyl chloride base matrix materials. Moreover, it has been noted that the nanoparticles increase the conduction current in nanocomposites specimens compared with the traditional polyvinyl chloride dielectrics.

Under nonuniform electric fields, Figs. 7–9 illustrate the dielectric strength breakdown characterization of pure and nanocomposite polyvinyl chloride industrial materials. It has been observed that adding individual nanoparticles (Clay, ZnO and $BaTiO_3$) raising dielectric strength of polyvinyl chloride, especially, in the case of adding two different types of nanoparticles together in polyvinyl chloride base matrix materials. Therefore, the conduction current decreases in polyvinyl chloride nanocomposites specimens compared with the traditional polyvinyl chloride material.

6. PD Simulation and Characterization

The effects of nanoparticles in developing the behavior of single-core power cable with existing different shapes (cylinder–sphere–ellipse) of voids (air–water–impurity) have

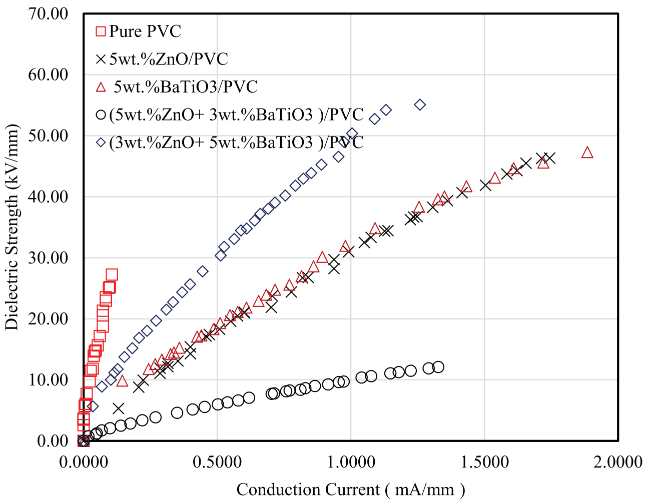

Fig. 6. Dielectric strength of nanocomposite insulation material containing ZnO and $BaTio_3$ nanoparticles under uniform electric fields.

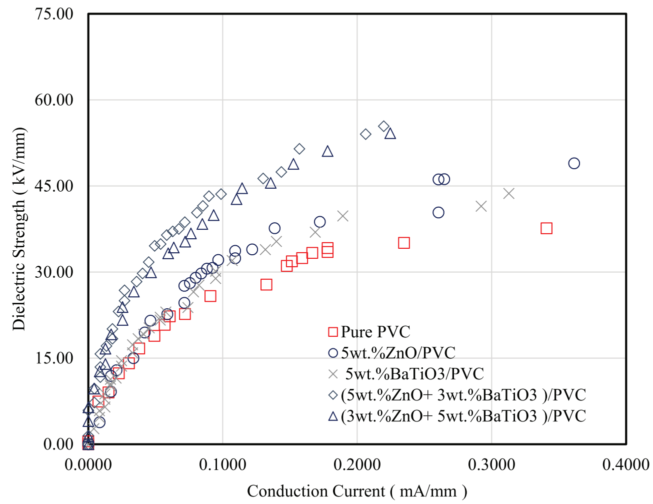

Fig. 8. Dielectric strength of nanocomposite insulation material containing ZnO and $BaTio_3$ nanoparticles under nonuniform electric fields.

been illustrated the importance of recent nanotechnology techniques. Therefore, the electric field stress can be controlled by changing relative permittivity of insulator material by adding individual nanocomposite or multi-nanocomposite materials to insulator material.

6.1. *Effect of air void in nanocomposites and multi-nanocomposites*

Figures 10 and 11 illustrate the behavior of electric stress within variant polyvinyl chloride insulation materials pure and nanocomposites that are containing different shapes of air voids. It has been observed that the electric field distribution within (cylinder, sphere and ellipse) air voids inside the insulation of single-core power cable has been decreased, whatever, the electric field distribution inside power cable insulation has been increased by adding Clay and ZnO nanoparticles due to low dielectric constant. And so, increasing the concentration of Clay nanoparticles causes more efficient effect for decreasing electric field distribution within (cylinder, sphere and ellipse) air voids but it is observed different behaviors to electric stress performance in the case of

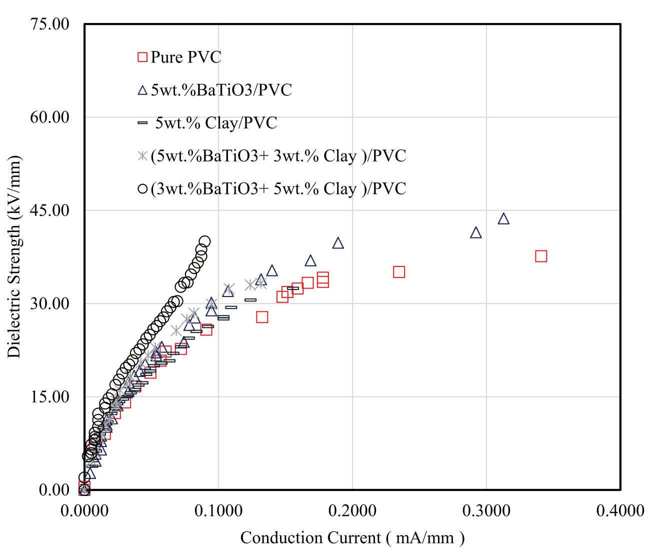

Fig. 7. Dielectric strength of nanocomposite insulation material containing Clay and $BaTio_3$ nanoparticles under nonuniform electric fields.

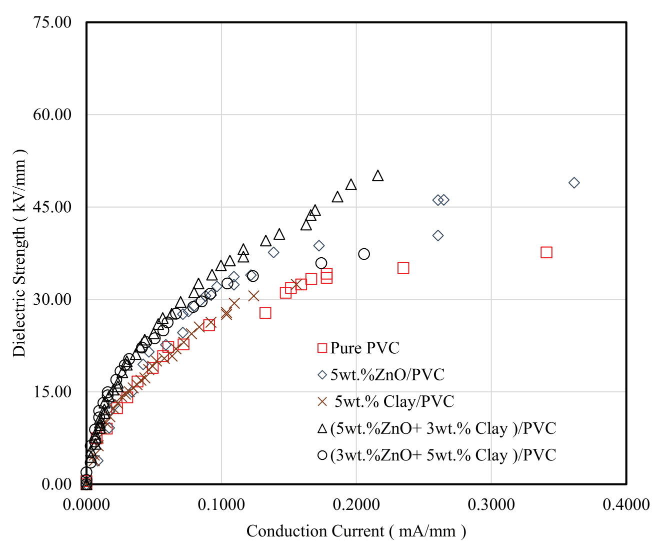

Fig. 9. Dielectric strength of nanocomposite insulation material containing Clay and ZnO nanoparticles under nonuniform electric fields.

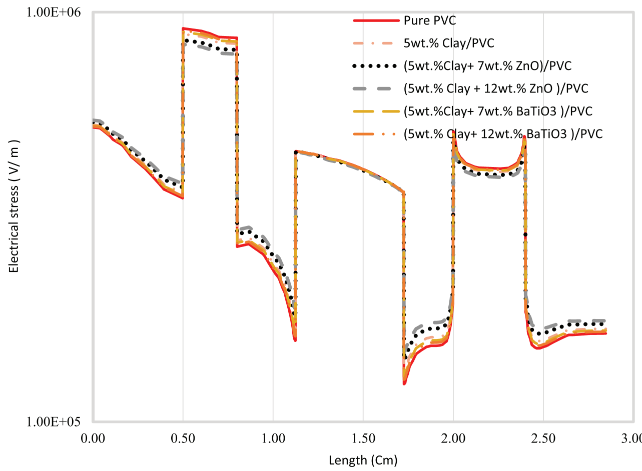

Fig. 10. Stress distribution in cable insulation with different air voids (cylinder–sphere–ellipse) compare 5 wt.% multiple nano composites/PVC.

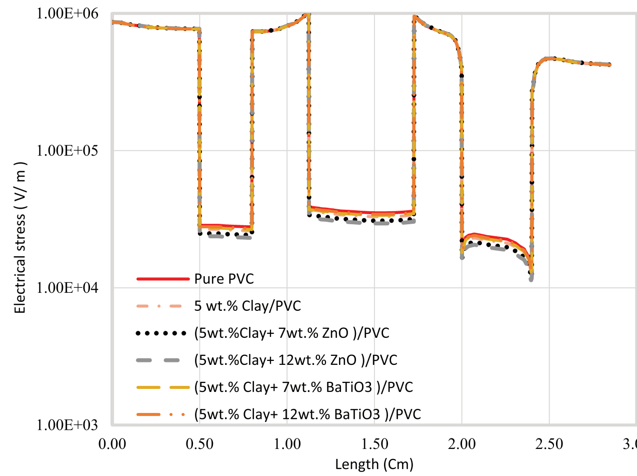

Fig. 12. Stress distribution in cable insulation with different water voids (cylinder–sphere–ellipse) in PVC nanocomposites.

adding multiple nanoparticles inside polyvinyl chloride. In a specific detail, Table 3 depicts the stress values of electric fields distribution in nanocomposites insulation of power cable with air different voids (cylinder, sphere and ellipse).

6.2. *Effect of water void in nanocomposites and multi-nanocomposites*

Figures 12 and 13 illustrate the behavior of electric stress within variant polyvinyl chloride insulation materials pure and nanocomposites in the case of presence water void. It has been obvious that the electric field distribution within (cylinder, sphere and ellipse) water voids inside the insulation of single-core power cable has been decreased and the electric field distribution inside power cable insulation has been increased by adding Clay and ZnO nanoparticles due to low dielectric constant. And so, increasing the concentration of Clay nanoparticles causes more efficient effect for decreasing electric field distribution within (cylinder, sphere and ellipse) water voids but it is observed different behaviors to electric stress performance in the case of adding multiple nanoparticles inside polyvinyl chloride. For a specific detail, Table 4 depicts the stress values of electric field distribution in nanocomposites insulation of single-core power cable with water different voids (cylinder, sphere and ellipse).

6.3. *Effect of impurities in nanocomposites and multi-nanocomposites*

Figures 14 and 15 illustrate the behavior of electric stress within variant polyvinyl chloride insulation materials pure

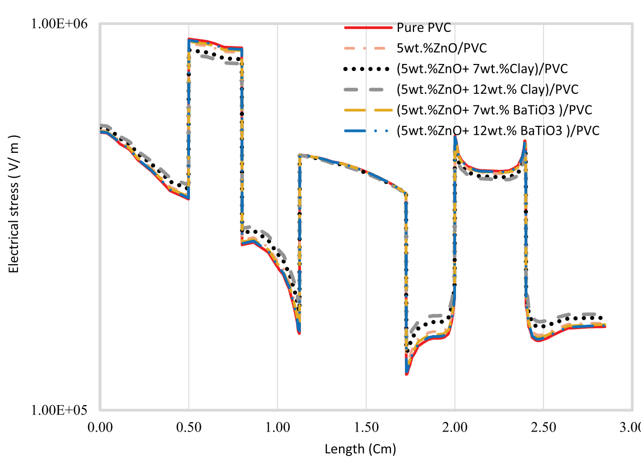

Fig. 11. Stress distribution in cable insulation with different air voids (cylinder–sphere–ellipse) compare 5 wt.% multiple nano composites/PVC.

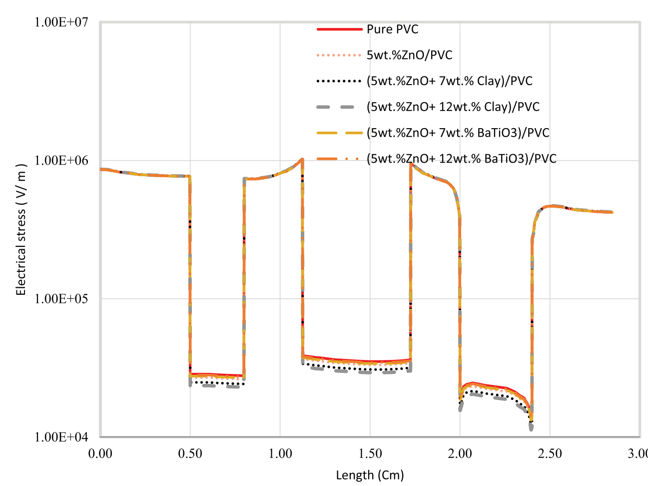

Fig. 13. Stress distribution in cable insulation with different water voids (cylinder–sphere–ellipse) in PVC nanocomposites.

Table 4. Stress distribution in cable insulation with different water voids.

Materials	E_{max} within cable insulation (V/m)	E_{min} within impurity cylinder void (V/m)	E_{min} within impurity sphere void (V/m)	E_{min} within impurity ellipse void
5 wt.% Clay/PVC	8.62E+05	2.60E+04	3.39E+04	1.77E+04
(5 wt.% Clay + 7 wt.% ZnO)/PVC	8.63E+05	2.42E+04	3.17E+04	1.65E+04
(5 wt.% Clay + 12 wt.% ZnO)/PVC	8.64E+05	2.31E+04	3.03E+04	1.57E+04
(5 wt.% Clay + 7 wt.% $BaTiO_3$)/PVC	8.62E+05	2.66E+04	3.47E+04	1.81E+04
(5 wt.% Clay + 12 wt.% $BaTiO_3$)/PVC	8.62E+05	2.71E+04	3.53E+04	1.84E+04
5 wt.% ZnO/PVC	8.62E+05	2.63E+04	3.43E+04	1.79E+04
(5 wt.% ZnO + 7 wt.% Clay)/PVC	8.63E+05	2.42E+04	3.17E+04	1.65E+04
(5 wt.% ZnO + 12 wt.% Clay)/PVC	8.64E+05	2.30E+04	3.02E+04	1.56E+04
(5 wt.% ZnO + 7 wt.% $BaTiO_3$)/PVC	8.62E+05	2.69E+04	3.51E+04	1.83E+04
(5 wt.% ZnO + 12 wt.% $BaTiO_3$)/PVC	8.61E+05	2.73E+04	3.56E+04	1.86E+04

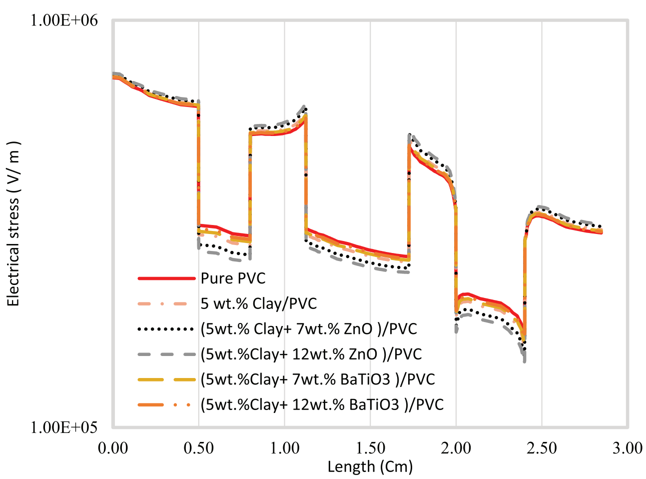

Fig. 14. Stress distribution in cable insulation with different solid impurities voids (cylinder–sphere–ellipse) in PVC nanocomposites.

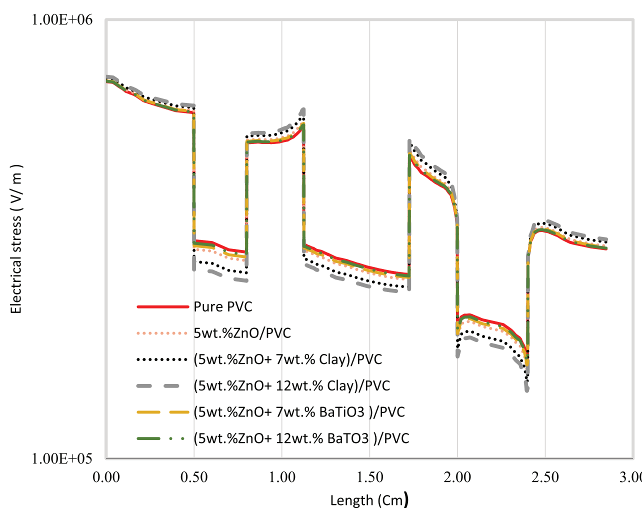

Fig. 15. Stress distribution in cable insulation with different solid impurities voids (cylinder–sphere–ellipse) in PVC nanocomposites.

and nanocomposites in the case of presence Copper impurity void. It has been observed that the electric field distribution within (cylinder, sphere and ellipse) Copper impurity voids inside the insulation of single-core power cable has been decreased and the electric field distribution inside power cable insulation has been increased by adding Clay and Zno nanoparticles due to low dielectric constant. And so, increasing the concentration of Clay nanoparticles causes more efficient effect for decreasing electric field distribution within (cylinder, sphere and ellipse) Copper impurity voids but it is observed different behaviors to electric stress performance in the case of adding multiple nanoparticles inside polyvinyl chloride. Moreover, Table 5 depicts the stress values of electric fields distribution in nanocomposites insulation of single-core power cable with Impurity different voids (cylinder, sphere and ellipse).

7. Trends of Nanoparticles Selection

The arrangement of multiple nanoparticles is an important parameter that is affected on increasing or decreasing the electric field distribution within different voids shapes (cylinder, sphere and ellipse) of air, water and impurities.[10,14,21,31] Also, it is cleared that using multiple nanoparticles technique is better than individual nanoparticle technique for decreasing electrostatic field inside different voids (air, water and impurities). It is deduced that clay and zinc oxide are the best nanoparticles for reducing the electric distribution inside (cylinder, sphere and ellipse) air voids. Finally, it is deduced that clay and zinc oxide are the best nanoparticles that are made a reduction in the electric distribution inside copper impurity voids. Selection of nanoparticles type depends on the appropriate properties (electric, dielectric,

Table 5. Stress distribution in cable insulation with different copper impurities.

Materials	E_{max} within cable insulation (V/m)	E_{min} within impurity cylinder void (V/m)	E_{min} within impurity sphere void (V/m)	E_{min} within impurity ellipse void
5 wt.% Clay/PVC	7.29E+05	2.80E+05	2.55E+05	1.88E+05
(5 wt.% Clay + 7 wt.% ZnO)/PVC	7.36E+05	2.65E+05	2.46E+05	1.78E+05
(5 wt.% Clay + 12 wt.% ZnO)/PVC	7.41E+05	2.55E+05	2.41E+05	1.72E+05
(5 wt.% Clay + 7 wt.% $BaTiO_3$)/PVC	7.27E+05	2.86E+05	2.58E+05	1.19E+05
(5 wt.% Clay + 12 wt.% $BaTiO_3$)/PVC	7.25E+05	2.90E+05	2.60E+05	1.94E+05
5 wt.% ZnO/PVC	7.28E+05	2.83E+05	2.56E+05	1.60E+05
(5 wt.% ZnO + 7 wt.% Clay)/PVC	7.36E+05	2.65E+05	2.46E+05	1.49E+05
(5 wt.% ZnO + 12 wt.% Clay)/PVC	7.41E+05	2.54E+05	2.40E+05	1.43E+05
(5 wt.% ZnO + 7 wt.% $BaTiO_3$)/PVC	7.26E+05	2.88E+05	2.59E+05	1.64E+05
(5 wt.% ZnO + 12 wt.% $BaTiO_3$)/PVC	7.24E+05	2.92E+05	2.61E+05	1.66E+05

mechanical, physical, etc.) that are awarded to be preferable, whatever the nanoparticles percentage depends on volume concentration of base matrix polymer. The type and percentage selection of nanoparticles should be not affecting the essential construction of polymer base matrix materials (1 wt.%–10 wt.%).

8. Conclusions

- Experimental tests deduced that adding individual nanoparticles (Clay, ZnO and $BTiO_3$) are raising dielectric strength of polyvinyl chloride under uniform and nonuniform electric fields, especially, in the case of adding two different types of nanoparticles together in polyvinyl chloride base matrix materials. In uniform electric fields, the conduction current increases in nanocomposites specimens compared with the traditional polyvinyl chloride material but the conduction current decreases in nanocomposites specimens compared with the traditional polyvinyl chloride material in the case of nonuniform electric fields.
- The addition of individual nanoparticles (Clay and ZnO) to polyvinyl chloride has changed the electrical insulation properties; thus, the nanoparticles decreased and increased electric field distribution inside power cable insulation based on their physical properties. Adding individual nanoparticle (Clay and ZnO) made a reduction in the electrostatic field distribution inside any voids (air, water, impurity) belt in polyvinyl chloride. On the other hand, the multi-nanoparticles technique has been given more ability for controlling in electrical properties of insulation, thus, it can be easily controlled in the electrostatic field distribution inside the insulation of single-core power cables.

Acknowledgment

The present work was supported by the Nanotechnology Research Center at Aswan University that is established by aiding the Science and Technology Development Fund (STDF), Egypt, Grant No: Project ID 505, 2009-2011.

References

[1] G. C. Crichton, P. W. Karlsson and A. Pedersen, Partial discharges in ellipsoidal and spherical voids, *IEEE Trans. Electr. Insul.* **24**(2), 335 (1989).

[2] R. J. Van Brunt, Physics and chemistry of partial discharges and corona, *IEEE Trans. Dielectr. Electr. Insul.* **1**(5), 761 (1994).

[3] C. Stancu, P. V. Notingher, F. Ciuprina *et al.*, Computation of the electric field in cable insulation in the presence of water trees and space charge, *IEEE Trans. Indus. Appl.* **45**(1), 30 (2009).

[4] A. Nosseir, Calculation of discharge inception voltage due to the presence of voids in power cables, *IEEE Trans. Electr. Insul.* EI-**14**(2), 117 (1979).

[5] A. Thabet and Y. A. Mubarak, The effect of cost-fewer nanoparticles on the electrical properties of polyvinyl chloride, *Electr. Eng. J.* **99**(2), 625 (2017).

[6] R. C. Smith, C. Liang, M. Landry *et al.*, The mechanisms leading to the useful electrical properties of polymer nanodielectrics, *IEEE Trans. Dielectr. Electr. Insul.* **15**(1), 187 (2008).

[7] A. Thabet and A. A. Ebnalwaled, Improvement of surface energy properties of PVC nanocomposites for enhancing electrical applications, *J. Int. Meas. Confed.* **110**, 78 (2017).

[8] S. Li, D. Xie and Q. Lei, Understanding insulation failure of nanodielectrics: Tailoring carrier energy, *High Volt.* **5**(6), 643 (2020).

[9] A. Thabet, M. Allam and S. A. Shaaban, Investigation on enhancing breakdown voltages of transformer oil nanofluids using multi-nanoparticles technique, *IET Gener. Transm. Distrib. J.* **12**(5), 1171 (2018).

[10] A. Thabet, N. Salem and E. E. M. Mohamed, Modern insulations for power cables using multi-nanoparticles technique, *Int. J. Electr. Eng. Inform.* **10**(2), 271 (2018).

[11] S. Diaham, Modulation of the dielectric breakdown strength in polyimide nanocomposites by deep traps tailoring in interphase regions, *IEEE Trans. Dielectr. Electr. Insul.* **26**(1), 247 (2019).

[12] J. Xue, Y. Li, J. Dong *et al.*, Surface charge transport behavior and flashover mechanism on alumina/epoxy spacers coated by SiC/

epoxy composites with varied SiC particle size, *J. Phys. D: Appl. Phys.* **53**, 155503 (2020).

[13]D. Ai, H. Li, Y. Zhou *et al.*, Tuning nanofillers in situ prepared polyimide nanocomposites for high-temperature capacitive energy storage, *Adv. Energy Mater.* **28**, 1903881 (2020).

[14]A. Thabet and N. Salem, Experimental progress in electrical properties and dielectric strength of polyvinyl chloride thin films under thermal conditions, *Trans. Electr. Electron. Mater. J.* **21**(1), 1 (2019).

[15]Nexans Energy Networks Company, 6-36 kV Medium Voltage underground power cables XLPE insulated cables catalogue, www.nexans.co.uk.

[16]M. Alsharif, P. A. Wallace, D. M. Hepburn and C. Zhou, FEM modelling of electric field and potential distributions of MV XLPE cables containing void defect, *COMSOL Conf.* (Milan, 2012), pp. 1–4.

[17]VEGA Grieshaber KG, List of dielectric constants catalogue, www.vega.com.

[18]S. Patel, S. Chaudhari and M. Patel, Analysis of electric stress in high voltage cables containing voids, *Int. J. Eng. Res. Technol*. **3**(3), 1443, 2014.

[19]M. Todd and F. Shi, Molecular basis of the interphase dielectric properties of microelectronic and optoelectronic packaging materials, *IEEE Trans. Compon Packag. Technol.* **26**(3), 667 (2003).

[20]A. Thabet, Y. Mobarak, N. Salem and A. El-Noby, Performance comparison of selection nanoparticles for insulation of three core belted power cables, *Inter. J. Electri. Comput. Eng.* **10**(3), 2779 (2020).

[21]A. T. Mohamed, Design and investment of high voltage nanodielectrics (IGI Global, 2020).

[22]K. K. Karkkainen, A. H. Sihvola and K. I. Nikoskinen, Effective permittivity of mixtures: Numerical validation by the FDTD method, *IEEE Trans. Geosci. Remote Sens.* **38**, 1303 (2000).

[23]A. Thabet and N. Salem, Optimizing dielectric characteristics of electrical materials using multi-nanoparticles technique, *IEEE, Int. Middle East Power System Conf. (MEPCON)* (Menofia, Egypt, 2017), pp. 220–225.

[24]G. Polizos, E. Tuncer, I. Sauers and K. L. More, Properties of a nanodielectric cryogenic resin, *Appl. Phys. Lett.* **96**(15), 152903 (2010).

[25]N. Tagami, M. Hyuga, Y. Ohki, T. Tanaka, T. Imai, M. Harada and M. Ochi, Comparison of dielectric properties between epoxy composites with nanosized clay fillers modified by primary amine and tertiary amine, *IEEE Dielectr. Electr. Insul. Trans.* **17**(1), 214 (2010).

[26]M. Todd and F. Shi, Characterizing the interphase dielectric constant of polymer composite materials: Effect of chemical coupling agents, *J. Appl. Phys.* **94**, 4551 (2003).

[27]Y. Yi and M. Sastry, Analytical approximation of the two-dimensional percolation threshold for fields of overlapping ellipses, *Phys. Rev. E* **66**, 066130 (2002).

[28]A. Thabet, Theoretical analysis for effects of nanoparticles on dielectric characterization of electrical industrial materials, *Electr. Eng.* **99**(2), 487 (2017).

[29]A. Thabet and Y. A. Mobarak, Dielectric characteristics of new nano-composite industrial materials, *Int. Conf. High Voltage Engineering and Application "ICHVE"* (New Orleans, USA, 2010), pp. 568–571.

[30]A. Thabet and N. Salem, Experimental investigation on dielectric losses and electric field distribution inside nanocomposites insulation of three-core belted power cables, *Adv. Indus. Eng. Polym. Res.* **4**(1), 1857 (2021).

[31]A. T. Mohamed, *Emerging Nanotechnology Applications in Electrical Engineering* (IGI Global 2021).

[32]C. Jeffrey Brinker and G. W. Scherer, *Sol-Gel Science: The Physics Chemistry of Sol-Gel Processing* (Academic Press, Inc., 1990).

[33]L. Bois, F. Chassagneux, S. Parola and F. Bessueille, Growth of ordered silver nanoparticles in silica film mesostructured with a triblock copolymer PEO–PPO–PEO, *J. Solid-State Chem.* **182**, 1700 (2009).

[34]H. N. Azlinaa, J. N. Hasnidawania, H. Norita and S. N. Surip, Synthesis of SiO_2 nanostructures using sol-gel method, *5th International Science Congress & Exhibition APMAS2015*, Vol. 129 (Lykia, Oludeniz, 2016), pp. 842–844.

[35]B. Reddy, *Advances in Nanocomposites — Synthesis, Characterization and Industrial Applications* (Intech Open, 2011), pp. 323–340.